

Swelling properties of roasted coffee particles

Verena Bernadette Hergarten,  Michael Kuhn and Heiko Briesen*

Abstract

BACKGROUND: In this study, the swelling behavior of roasted coffee particles in water and particularly its impact on particle diameter is examined by applying laser-diffraction analysis and microscopy. Several potential influencing factors are investigated: initial particle size, roasting degree, and temperature. Additionally, the time dependency of swelling and particle shape is evaluated at two different temperatures.

RESULTS: We verify that particle erosion occurs – as observed by an increase of the fine particle fraction after wetting – and it is revealed that this effect is more pronounced with a rise in temperature. The total relative increase in particle size is determined as approximately 15% based on a broad range of different sized coffee grounds. It is demonstrated that the degree of swelling is independent of both the initial particle diameter and the roasting degree. The particle shape is found to be unaffected by swelling. This research reveals that swelling is initially quick, with 60–80% of the final steady-state diameter being reached after 30 s and completed after 4 min of wetting, i.e. within the timescale of conventional coffee brewing methods.

CONCLUSION: This work provides a better understanding of the impact of wetting as part of the coffee brewing process, thus aiding the design, modeling, and optimization of coffee extraction. It clarifies the strong deviation of previous results on coffee-particle swelling by considering particle erosion and degassing and provides a robust method for quantification.

© 2020 The Authors. *Journal of The Science of Food and Agriculture* published by John Wiley & Sons Ltd on behalf of Society of Chemical Industry.

Keywords: erosion; extraction; imbibition; particle size; wetting

INTRODUCTION

In recent decades, researchers have become increasingly interested in coffee extraction. In particular, the highly complex process of percolation conducted for espresso preparation has not been fully explored, a process that combines the mass transport of multiple volatile and non-volatile substances with flow through an inhomogeneous particle packing.

Variations in brewing parameters strongly influence the extraction yield, the composition, and hence the sensory profile of the coffee beverage.¹ Besides water pressure,² temperature,³ coffee/water ratio,⁴ extraction method,⁵ and water quality,⁶ it is known that the particle size distribution of ground roasted coffee beans is an essential variable affecting not only the diffusion of solutes into water but also the flow through the particle bed. Voilley and Simatos⁷ showed that a finer coffee ground leads to a higher dissolved solids content. Spiro and Selwood⁸ revealed an effect of the particle diameter on the extraction kinetics of caffeine for coffee infusion by demonstrating that with decreasing particle size, the rate constants of caffeine extraction increased by two orders of magnitude. Furthermore, it applies to percolation that the size of coffee particles is positively correlated to the permeability of the particle bed according to the Kozeny–Carman equation; particle size distribution and particle shape also affect permeability by means of the pore size distribution and tortuosity.⁹ According to Darcy's law,⁹ the flow velocity rises with increased permeability and results in a shorter residence time corresponding to a lower extraction yield, as verified for espresso extraction by Kuhn

et al.;¹⁰ they also discovered that extraction kinetics, and thus, the ratio of compounds in the final beverage, are influenced by the particle size distribution.

It has often been stated in the literature that swelling of coffee particles has a considerable impact on coffee extraction. This swelling process is described as an effect occurring with colloidal imbibition, which means the uptake of water by plant tissue followed by chemical hydration of the biocolloids present in the cell and an expansion of the insoluble cell wall structure.^{11,12} Compounds that are abundant in roasted coffee and are assumed to contribute to swelling due to their hydrophilicity¹³ are water-insoluble polysaccharides, referred to as holocellulose.

Three principal polysaccharides have been identified in green coffee: arabinogalactan,¹⁴ mannan,¹⁵ and cellulose.¹⁶ Their structure and contents were analyzed by Bradbury and Halliday,¹⁷ who found similar contents of mannan and cellulose in arabica and robusta beans: 2.2 g kg⁻¹ mannan and 0.8 g kg⁻¹ cellulose. The arabinogalactan content is slightly higher in robusta beans at 1.7 g kg⁻¹, with 1.4 g kg⁻¹ in arabica beans. During roasting, holocellulose polysaccharides are thermally degraded.¹⁸ The total

* Correspondence to: H Briesen, Chair of Process Systems Engineering, TUM School of Life Sciences, Technical University of Munich, Gregor-Mendel-Straße 4, D-85354 Freising, Germany. E-mail: heiko.briesen@tum.de

Chair of Process Systems Engineering, TUM School of Life Sciences, Technical University of Munich, Munich, Germany

content decreases from approximately 3.2 g kg^{-1} on a dry basis to 2.5 g kg^{-1} when light roasted, 1.9 g kg^{-1} when medium roasted, and 1.7 g kg^{-1} when dark roasted, whereby cellulose remains the most stable throughout the roasting process.¹⁸ Asante and Thaler¹⁹ demonstrated that the water solubility of mannan increases during the roasting process, leading to a decrease in the insoluble fraction of the bean and an increase in the viscosity of the beverage.²⁰ Due to this change in the amount of insoluble polysaccharides, it can be assumed that the roasting degree influences swelling. Furthermore, it is understood that the swelling of pulp fibers composed of cellulose, lignin, and hemicellulose is influenced by pH and salt content,²¹ lignin content,²² temperature,²³ hemicellulose,²³ and fibrillar content.²⁴ Cuissinat and Navard²⁵ revealed that plant fibers mainly composed of cellulose and hemicellulose and small contents of lignin and pectin exhibited homogeneous swelling without dissolution in 0.76 g kg^{-1} sodium hydroxide (NaOH) and in most aqueous *N*-methylmorpholine-*N*-oxide (NMMO) solutions. The ratio of swelling decreased with lower concentrations of the solvent. According to Wolfrom *et al.*,¹⁵ mannan is partially soluble in a 1.8 g kg^{-1} aqueous NaOH solution. Based on these findings on the individual insoluble polysaccharides comprising the coffee matrix, the occurrence of swelling in water is basically presumable but possibly depends on the composition of coffee ground and solvent.

Rivetti *et al.*²⁶ concluded that swelling is influenced by water alkalinity resulting in an increase in percolation time. They demonstrated by means of discriminant analysis that alkalinity has a significant effect on the swelling of coffee particles using particle-size-distribution measurements; however, they did not present data concerning the quantitative size increase of particles. Measurements of particle size and particle size distribution have been applied by several other authors during recent decades, but their results differ widely. Sivetz and Desrosier²⁷ reported a size increase of 7% based on microscopy measurements without presenting any information about the applied method and the initial particle size. Spiro *et al.*²⁸ determined an increase in size of $20 \pm 4\%$ for green coffee and an increase of $17 \pm 5\%$ for roasted coffee with an initial mean diameter of 1.072 and 0.994 mm respectively. Measurements were limited to relatively large particles and visual inspection, which does not enable a conclusion to be drawn for smaller particles applied for espresso and drip coffee brewing. The swelling of single particles was questioned by Hinz *et al.*²⁹ and Steer³⁰ as they reported a volume increase for whole coffee beans and pressed tablets of coffee particles but no increase regarding individual particles under the microscope. Furthermore, Hinz³¹ determined the particle size distribution by laser-diffraction analysis of coffee particles after different periods of extraction. An increase in the fine fraction of particles $< 250 \mu\text{m}$ was detected along with a slight shift of coarser particles toward larger particle sizes. In that work, no dispersing unit was mentioned, but Hinz states that the moisture contents of the measured particles were between $0.047 \times 10^{-3} \text{ g kg}^{-1}$ and $1.847 \times 10^{-3} \text{ g kg}^{-1}$, indicating that moist particles were measured in an air stream. As the particle size differs with varying moisture content, there are advantages to measuring particle size distribution in an aqueous medium to eliminate this degree of freedom. Such measurements in a wet state were applied by Mateus *et al.*,¹³ who found an increase of the $d_{4,3}$ by 20–23% 10 to 15 min after wetting. They measured particles with an initial size of 750 and 1050 μm and they also demonstrated (by using scanning electron microscopy) that water

penetrated into the cell lumen, which supports the hypothesis that imbibition occurs.

Finer particles were analyzed by Corrochano,³² who compared laser-diffraction measurements of dry and wet particles by dispersing them in an air stream and in tap water at $15 \text{ }^\circ\text{C}$. He revealed that the fine particle fraction is higher when using the wet method compared with the dry and that the wet method detects finer particles. These fine particles are assumed to be fine cell fragments that are either detached from the coffee-particle's pores or are lumps of substances that are insoluble at the measuring temperature, but which are possibly soluble at higher temperatures. Comparing the $d_{4,3}$ of two roasted coffee grounds, Corrochano found a volume increase in the $d_{4,3}$ of 12% for medium-coarse particles with an initial $d_{4,3}$ of $363.6 \pm 3.8 \mu\text{m}$, but no significant increase in the $d_{4,3}$ for fine particles with an initial $d_{4,3}$ of $198.8 \pm 0.9 \mu\text{m}$. According to Corrochano, the strong deviation from Mateus *et al.*'s¹³ results might be attributed to a different dispersant or the roasting degree. The absence of significant swelling of fine particles in Corrochano's work may lead to the assumption that the degree of swelling depends on the initial size of coffee particles. Accordingly, this aspect is addressed in this study.

It is clear from the widely differing values and contradictory statements mentioned earlier that no consensus exists about the occurrence and degree of coffee-particle swelling. Additionally, relevant factors – such as the initial particle size, the roasting degree, and temperature – have not been investigated sufficiently. This work aims to clarify the effect of water on the particle dimensions of ground roasted coffee in a statistically significant and reproducible way; it considers the entire range of grinding degrees applied in common brewing methods as well as the influences of temperature and the degree of roasting. The effect of water quality, i.e. alkalinity/acidity and mineral content is not considered in this article. In addition to laser-diffraction measurements of sieved samples, microscopy is applied to assess the time evolution of swelling and its relevance for different extraction techniques.

With regard to the influence of temperature on swelling, Spiro and Chong³³ state that swelling is more pronounced at elevated temperatures but indicate that obtaining quantitative measurements was challenging. Through microscopy measurements of single particles at two different temperatures (25 and $80 \text{ }^\circ\text{C}$), this study investigates the effect of temperature on both the rate and the degree of swelling.

MATERIALS AND METHODS

Roasted coffee

The medium-roast coffee (of a single origin from Marcala, Honduras, 100% arabica, organic certified DE-ÖKO-039) was supplied in 250 g packages (of a synthetic polymer with an aluminum barrier and a one-way degassing valve) by a local roaster (Fausto Kaffeerösterei GmbH, Munich, Germany). The light-roast coffee (of mixed origin from Colombia, South America and Tanzania, Africa, 100% arabica, rainforest alliance certified) was a product called Blonde Roast (produced by Tchibo GmbH, Bremen, Germany), which was packed in 250 g packages (of low-density polyethylene with aluminum barrier and no degassing valve). Both raw materials are depicted in Fig. 1. From visual comparison with images presented by Wang and Lim,³⁴ the roasting degree of both products is estimated to be between the first and second crack, i.e. within a conventional range for customary roast coffee.



Figure 1 Light roast (left) and medium roast (right) coffee beans.

Grinding and sieving

The coffee was ground using a professional grinder (Mahlkönig EK 43, Hemro Manufacturing Germany GmbH, Hamburg, Germany) equipped with cast steel grinding disks and a continuous dial for grind adjustment (scaled between 1–11 in increments of 0.1). Good reproducibility of grinding was confirmed in preliminary experiments. To prevent contamination of the grinder with residual particles, a small amount of coffee was ground and discarded before collecting the samples. The coffee was ground at settings of 2.0 (fine), 5.0 (medium), and 8.0 (coarse), which are subsequently referred to as grinding degree. Directly after grinding, the coffee was partially sieved in a vibrational sieving tower (AS 200, RETSCH GmbH, Haan, Germany). Approximately 50 g of ground coffee was sieved continuously for 10 min at an amplitude of 1.2 mm. Using a soft brush, agglomerates were separated and fine particles adhering to the sieves were detached. Subsequently, the sieving procedure was repeated as described earlier. In the case of grinding degree 2.0, vibrational sieving was conducted three times for 2 min at 10 s intervals, and between each sieving step the adhesion and cohesion of the particles was counteracted using the brush. The sieves used and the corresponding grinding settings and fractions, described as F (fine), S (small), M (medium), and L (large), are listed in Table 1. Air jet screening (LPS 200 MC, RHEWUM GmbH, Remscheid, Germany) was applied to remove adhering fines from the particles and to further separate agglomerates. This was conducted for 5 min at an air flow of $70 \text{ m}^3 \text{ h}^{-1}$ and a rotation speed of 50 rpm.

Laser-diffraction analysis

Particle-size-distribution measurements were conducted with a laser-diffraction system (HELOS/BR, Sympatec GmbH, Clausthal-Zellerfeld, Germany). Particles were supplied and dispersed

either in a dry state by air pressure (VIBRI and RODOS, Sympatec GmbH) or in circulated, demineralized water (QUIXEL, Sympatec GmbH). Data from the detector were collected and evaluated (based on the Fraunhofer diffraction theory) by a compatible software (WINDOX Software, Sympatec GmbH). The measuring ranges of the lenses used for different fractions are shown in Table 1. Interval classification differs between the measuring ranges and along the scale of particle sizes with increasing interval sizes for larger particle fractions. Volume distributions were determined, i.e. the cumulative and density distribution of the volume of spheres with a diffraction-equivalent diameter. The volume density describes the difference quotient of the cumulative distribution for a specific particle size interval given by the measuring range.

For dry measurements, the sieved samples were split (DR 1000, RETSCH GmbH, Haan, Germany; Laborette Type 10.102, FRITSCH GmbH, Idar-Oberstein, Germany) to achieve homogeneous samples and weighed to ensure an equal sample weight of 10.00 g (FB6CCE-H, Sartorius AG, Göttingen, Germany). Three samples per sieving fraction were measured at a conveying speed of 80% relative to maximum speed and a primary pressure of 2.5 bar.

Wet measurements were conducted after particle-water contact of 20 min, after which the steady state of swelling was assumed.¹³ Briefly, 10 g of particles were immersed in 300 mL of boiled, demineralized water at a temperature of 90 °C on a heated magnetic stirrer and were stirred for 20 min. During this period, the temperature decreased to approximately 60 °C due to heat loss. To investigate the effect of extraction temperature, stirring was also performed at a temperature of 25 °C, following the same procedure. Subsequently, non-sieved samples from the stirred suspension were inserted directly into the dispersion unit of the laser-diffraction instrument with a Pasteur pipette. Before the analysis commenced, ultrasound was applied for 60 s to separate agglomerates; after a pause of 10 s, laser-diffraction measurements were conducted four times for 10 s with 5 s pauses in between. The pumping velocity in the system was 30% (relative to maximum velocity) for all experiments. In the case of the sieved particle fractions S, M, and L, the extracted coffee ground was separated from water in a 200 μm sieve and washed for 5 min with demineralized water to remove the fine particles. This step was essential to approximate monomodal particle size distributions, which are necessary for accurate quantification of differences and to exclude the effects of particle erosion and fluctuations in optical density throughout the measurements. After adding the coffee particles to the dispersant and waiting 5 min to reach a constant optical density, measurement commenced. For a period of 120 s, diffraction was analyzed; the measurement was repeated

Table 1. Specification of grinding and sieving settings and corresponding measuring range of laser diffraction analysis

Sieving	Grinding degree	Sieving range (μm)	Measuring range (μm)
None	2	—	0.5–1750
F ^a	2	< 200	0.5–875
S ^b	2	200–300	0.5–1750
M ^c	5	400–500	0.5–1750
L ^d	8	710–800	0.5 – 3500

^a F (fine).

^b S (small).

^c M (medium).

^d L (large).

four times with 5 s pauses. No ultrasound was used to avoid an undesired degradation of particles. Four to five samples were analyzed per sieved fraction, and three to five samples were analyzed from three ground batches with reference to the non-sieved samples. Weighted mean values and variances, outliers, and 95% confidence intervals (assumption of *t*-distribution) were calculated in Microsoft Excel 2016. Statistical analysis was conducted in MATLAB R2018a software using the functions *ttest2* and *ranksum* to identify significant differences between particle size classes. Additionally, the functions *fitlm* combined with *anova* were used to check for linear correlation. The relative diameter increase was calculated as:

$$\Delta d_{rel} = \frac{(d_f - d_0)}{d_0} \cdot 100\% \quad (1)$$

where d_f defines the final diameter of the swollen particle and d_0 the initial diameter. The relative diameter increase was determined for the diameters $d_{10,3}$, $d_{16,3}$, $d_{50,3}$, $d_{84,3}$, $d_{90,3}$, and $d_{99,3}$ which correspond to a specific quantile of the volume distribution, where the first index represents the respective quantile expressed in a percentage. This description must be distinguished from the De Brouckere mean diameter $d_{4,3}$ which defines the volume moment mean of the particle size distribution. Based on the calculations using Eqn (1) for the previously mentioned quantiles, the mean diameter increase and the respective standard deviation was calculated for different sized particles. Outliers, (occurring mostly for fine particles where the standard deviation was large) were excluded, but through comparison with the result for a complete data set, it was revealed that this did not change the mean value (see Results section).

Microscopy

A light microscope (BX51, OLYMPUS Corporation, Tokyo, Japan) was used for single-particle measurements. The microscope was equipped with a motorized revolving nosepiece (BX-REMCB & UHS, OLYMPUS Corporation), a scanning stage (SCAN, 130 × 85 travel range, 4 mm ball screw pitch, Märzhäuser Wetzlar GmbH & Co. KG, Wetzlar, Germany), a motorized focus drive (MFD-2, Märzhäuser Wetzlar GmbH & Co. KG), and a stepper motor controller connected to a joystick (TANGO 3 Desktop & 3-Axes Joystick, Märzhäuser Wetzlar GmbH & Co. KG). This enabled the fine adjustment of focus and table position. Images and videos were recorded using a high-resolution camera (XC50, OLYMPUS Corporation) and analyzed in a compatible software (analySIS, OLYMPUS Corporation).

To remove gas bubbles from the surface of coffee particles that appeared with degassing, a sealed flow cell was constructed from acrylic glass, which enabled the analysis of particles surrounded by water flow. Without removal, these gas bubbles would have disturbed the measurement of the projection area as they obscure the outline of particles. The coffee particles were affixed on a cover glass using a water-resistant, transparent, two-component adhesive (epoxy resins and amines, UHU GmbH & Co. KG, Bühl, Germany) and fixed inside the flow cell with transparent tape (tesafilm transparent, tesa SE, Norderstedt, Germany). The adhesive layer was spread as thin as possible to prevent immobilization of the particles in the direction of the projection plane. All particles analyzed were within the size range of 400 to 1000 μm , which reflects the coarse fraction of coffee grounds applied for drip and infusion brewing. Smaller particles were not measurable due to handling difficulties. Demineralized water

was pumped through at temperatures of approximately 80 and 25 °C at a flow rate of 50 to 80 mL min⁻¹ respectively using a peristaltic pump (TU/200, medorex e. K., Nörten-Hardenberg, Germany). Prior to each experiment, a beaker on a magnetic stirrer (serving as a water reservoir for the pump) was filled with fresh demineralized water; in the case of the measurements at 80 °C it was preheated with boiling demineralized water. The flow cell, hoses, and beaker were isolated with rubber foam (adhesive rubber tape 5 m × 50 mm × 3 mm, HORNBAACH Baumarkt AG, Bornheim, Germany; insulating tube and insulating mat: 9 mm insulating thickness, 6 mm tube diameter, Koste/Weitzel GbR, Wiesloch, Germany) to reduce heat loss. The temperature inside the flow cell (after passing through the beaker, pump, and hose) was 80 °C (temperature sensor: HI 98509, Hanna Instruments Inc., Woonsocket, RI, USA). A characteristic extraction temperature of 90 °C was not achieved due to heat loss despite insulation measures and preheating. Shortly before the water boundary surface had reached the particles, video recording commenced and then stopped after 150 s. Images were taken from this video for analysis after the beginning of wetting at 10, 20, 30, 40, 50, 60, 90, and 120 s, after which single images were regularly taken at defined time intervals. The water temperature in the beaker reached approximately 60 °C at the end of the experiment due to inevitable heat loss, yielding a temperature profile close to the extraction conditions described for laser-diffraction analysis (see earlier).

All photographs were transformed into binary images and the particles' projection area A_{proj} as well as the maximum and minimum Feret diameter $d_{F,max}$ and $d_{F,min}$ were determined. Any bubbles not removed by flow were separated from the particle outline using image processing. Based on the collected data, the projection-area-equivalent diameter of a circle d_{proj} was calculated as

$$d_{proj} = \sqrt{\frac{4}{\pi} A_{proj}} \quad (2)$$

and the aspect ratio AR was computed as the ratio of the minimum to the maximum Feret diameter, as follows:

$$AR = \frac{d_{F,min}}{d_{F,max}} \quad (3)$$

The relative diameter increase was determined according to Eqn (1) using d_{proj} at time t as diameter of the swollen particle and d_{proj} in the dry state ($t = 0$) as initial diameter. The progress of swelling was determined as

$$\text{Progress of swelling} = \frac{(d(t) - d_0)}{(d_f - d_0)} \cdot 100\% \quad (4)$$

where $d(t)$ is d_{proj} at time t and d_f is the final projection area equivalent diameter 20 min after the beginning of wetting.

RESULTS

Impact of swelling on the particle size distribution

As described, non-sieved medium-roast coffee grounds were analyzed at two different extraction temperatures: 25 and 90 °C. The volume distributions of these samples are presented in Fig. 2. The presented error bars represent 95% confidence intervals, which applies to all particle size distributions subsequently presented.

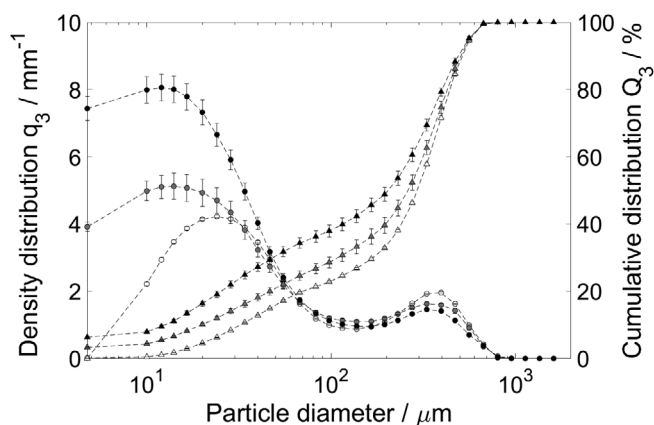


Figure 2 Density (○) and cumulative (△) distributions of non-sieved medium-roast coffee particles in dry state (white), wetted at 25 °C (gray) and wetted at 90 °C (black).

For better visibility of the fine fraction, the scaling of the abscissa is logarithmic. For clarity, it should be noted that the area of the density distribution does not represent the actual volume proportion due to its logarithmic transformation, i.e. the fine fraction is distinctly smaller than it appears from this plot. Each data point represents the middle of the respective particle size interval. For the dry coffee grounds, a bimodal distribution typical for coffee is recognizable with the first mode between 20 and 30 μm and the second at approximately 400 μm . Comparing the coffee grounds' distribution in dry and wet state, it is evident that the volume density for particles < 40 μm is significantly higher after wetting. For the coarse fraction, the volume density for particles > 250 μm is reduced for wet particles. This result is confirmed by a two-sample *t*-test and a Mann–Whitney U-test at the 1% significance level, summarized in Table A1 in the Appendix. In a wet state, both modes are shifted to smaller particle sizes; the first one is located at 12 μm and the second at 330 μm . Additionally, it is evident that very fine particles appear with the wet samples, which are small enough to exceed the lower threshold of the measuring range (< 10 μm). A further increase in the fine particle fraction can be seen with increased extraction temperature. With reference to the distribution of hot, extracted coffee grounds, the volume density of particles < 50 μm is significantly increased compared to the wet measurements at an extraction temperature of 25 °C and is simultaneously decreased in the range 90–500 μm (see Table A1, Appendix).

Figure 3 shows the particle size distributions of the sieving fractions F, S, M, and L (for specifications see Table 1) derived from medium-roast coffee grounds. The lines between values enable accurate readability of the individual distributions. A shift of the entire density and cumulative distribution toward larger particle sizes after wetting can be seen in the coarse fractions S, M, and L. This shift indicates a size increase of the particles. A small peak at the density distribution's left end is still visible for the wet dispersion. However, the proportion of these fine particles is small due to the washing action described earlier; therefore, their influence on the cumulative distribution can be neglected. This is not the case for the fine fraction F, where a strong increase in the volume density is still visible at the distribution's left end. A significant shift of the cumulative distribution on the right side of the mode is detected, and the mode itself shifts slightly from around 28 μm to 34 μm . Nonetheless, results in this size range must be

treated with caution as separation by means of sieving is not achieved with sufficient precision.

The relative diameter increase is plotted against the initial particle diameter in Fig. 4. Data from all particle fractions F, S, M, and L after the exclusion of three outliers ($d_{10,3}$ and $d_{50,3}$ of fraction F and $d_{99,3}$ of fraction S) is shown. The presented values result in a mean relative diameter increase of $15 \pm 4\%$. Including the complete dataset in the calculation yields a relative diameter increase of $15 \pm 7\%$. A linear regression coupled with an analysis of variance for the linear model's slope reveals no significant correlation between relative diameter increase and initial particle diameter (see Table A2, Appendix). Thus, it is concluded that the diameter increase is independent of the initial particle size when referring to the size range presented in Fig. 4.

To investigate possible effects from the type of roasting, measurements were repeated with a light-roast coffee, as described earlier. The dry and wet particle size distributions for sieving fractions F, S, and M are shown in Fig. 5. The same shift of the modes and cumulative distribution curves toward larger particle sizes is visible as for medium-roast coffee (see Fig. 3) with respect to sieving fractions S and M. Sieving fraction F does not exhibit a shift of the mode located at around 40 μm , but the cumulative distribution is shifted to the right for particles > 100 μm . It is assumed that the very fine particles located at the distribution's left end (which are not measured in a dry state due to their adherence on the larger particle's surface) are responsible for this difference compared to larger fractions where separation is feasible. The separation of agglomerates in a wet state might also be influential.

It is evident from Fig. 6 that the mean relative diameter increase for the sieved light-roast coffee ground is identical to that for medium-roast coffee at $15 \pm 3\%$ when the three extreme outliers $d_{10,3}$ and $d_{16,3}$ of fraction F and $d_{99,3}$ of fraction M are excluded. Including outliers slightly shifts the mean value to $13 \pm 10\%$. Additionally, no significant correlation is found between relative size increase and initial particle diameter, as shown in Table A2 in the Appendix. These results imply that the roasting degree does not significantly influence the degree of swelling if the water quality and temperature is kept constant.

Time dependency

Time courses of the relative diameter increase Δd_{rel} for individual particles, which were determined by microscopy according to Eqn (1), are presented in Fig. 7(a) for the medium-roast coffee and in Fig. 7(b) for the light-roast coffee. As the final relative diameter increase differs strongly for particles measured at the same conditions and exhibiting similar initial particle sizes, image analysis by microscopy is found to be an inappropriate method for the quantification of total swelling. In Table A3 (Appendix), statistical results are listed for the comparison of total swelling for different temperatures and roasts. No significant difference in the total size increase is found for different roasting degrees due to the strong deviation of measurements confirming the result from laser-diffraction analysis. Comparing the results determined at different water temperatures (80 versus 25 °C), no significant difference between the medium-roast and the light-roast coffee is evident, which is also based on the large scattering within both series of experiments. At 25 °C single, markedly higher diameter increases are measured for both roasts. However, this is possibly caused by the growth and adhesion of gas bubbles that could not be completely removed by water flow at lower temperatures and that had to be distinguished and subtracted from the particles

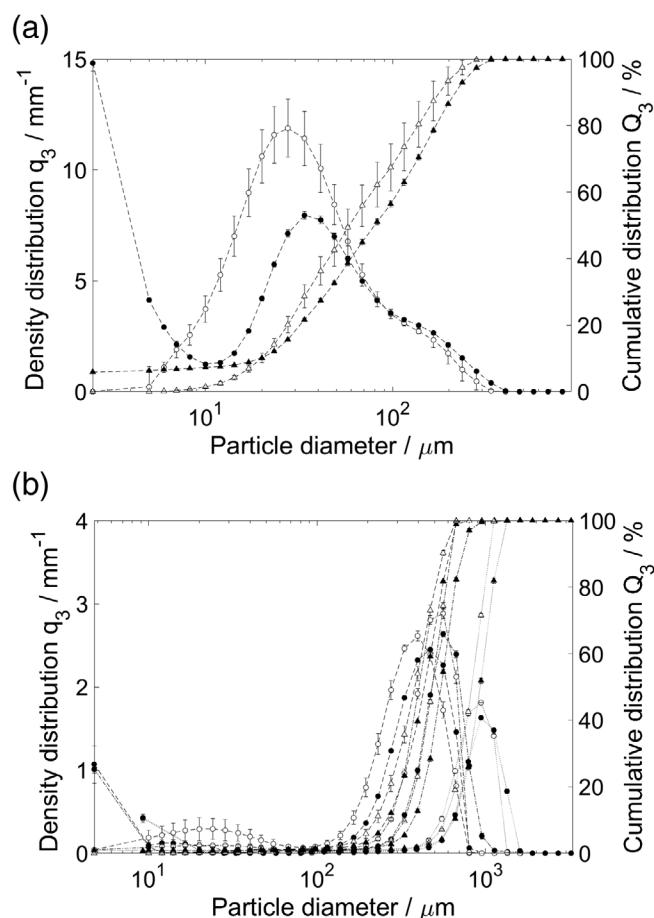


Figure 3 Density (○) and cumulative (△) distributions of sieved medium-roast coffee particles in dry state (white) and wetted at 90 °C (black). (a) Sieving fraction F (fine). (b) From left to right: sieving fractions S (small), M (medium), and L (large).

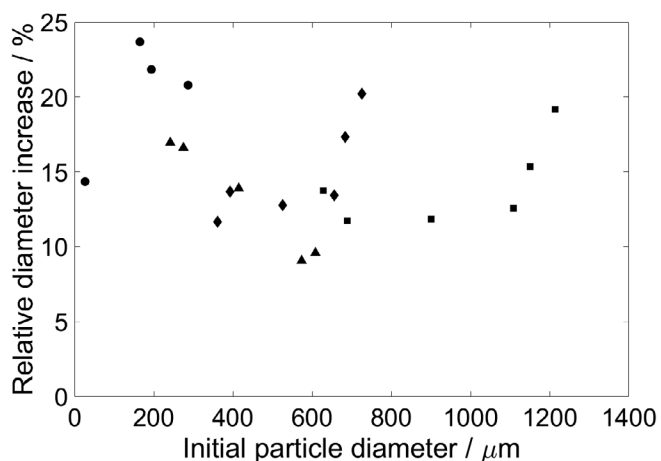


Figure 4 Relative diameter increase for medium-roast coffee versus initial particle diameters of sieving fractions F (fine) (●), S (small) (▲), M (medium) (◆), and L (large) (■).

during image processing. However, this could not guarantee the complete exclusion of undetected bubbles from the measured projection area. Two exemplary images showing light-roast particles before and after a wetting period of 20 min are presented in

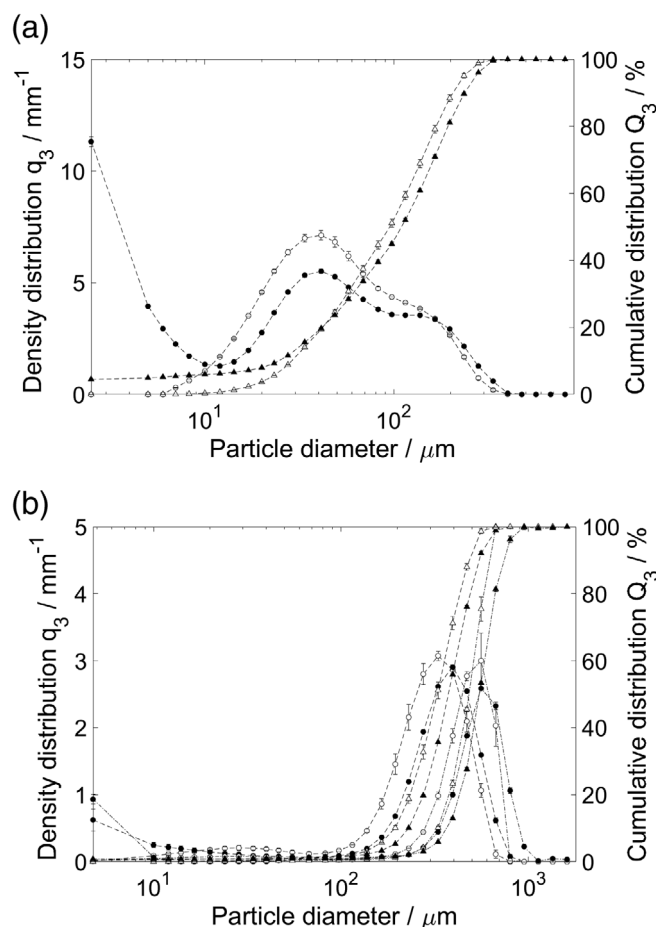


Figure 5 Density (○) and cumulative (△) distributions of sieved light-roast coffee particles in dry state (white) and wetted at 90 °C (black). (a) Sieving fraction F (fine). (b) From left to right: sieving fractions S (small), M (medium), and L (large).

Fig. 8. Large and small gas bubbles as well as cell fragments adhering to the particle surfaces are visible. Additionally, a detachment of small particles and color pigments carried away with the fluid flow was observed, complying with the increase in fines detected by laser diffraction analysis.

In addition to the particles' projection area, the minimal and maximal Feret diameter was determined and used for calculating the aspect ratio as a characteristic descriptor of particle shape (Eqn (3)). Figure 9 shows the aspect ratio of the same particles as depicted in Fig. 7, plotted over time. Most particles exhibit an aspect ratio between 0.6 and 0.8, visible for both roasts. This confirms that coffee particles within the measured size range are not spherical in shape but instead are flat and elongated. It is revealed by applying linear regression and analysis of variance (ANOVA) that no significant change occurs during swelling, as presented in Table A4 in the Appendix.

Figure 7 reveals that the final degree of swelling is reached within the first couple of minutes. Small decreases and fluctuations of the relative diameter increase are visible, but these are based on the experimental error from detaching fragments and gas bubbles. To investigate the time dependency of swelling, the progress of swelling described by Eqn (4) is shown for the first 5 min in Fig. 10. No clear distinction in terms of time dependency is possible when comparing different roasts and water temperatures due to the large differences between individual particles.

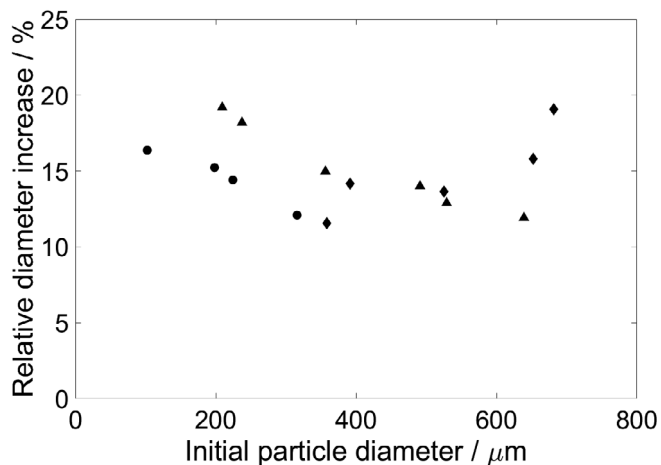


Figure 6 Relative diameter increase for light-roast coffee versus initial particle diameters of sieving fractions F (fine) (●), S (small) (▲), and M (medium) (◆).

The results for light-roast coffee show a broader scattering of the values for the first 100 s, which can be attributed to the slightly larger sample size. However, estimations about the status of swelling in the scope of characteristic brewing times are possible. Table 2 lists the average values for two conventional brewing times: 30 s as a typical residence time for espresso and 4 min as a usual contact time for infusion methods. After 30 s, around 83% of the final diameter is reached (on average) both at 80 and 25 °C for medium-roast coffee; the average for light-roast coffee is 71% and 59%, respectively. After 4 min of wetting, a steady state is reached. Values > 100% arise from relating the diameter increase to the diameter increase after 20 min (see Eqn (4)), which is subject to experimental error; therefore, it is partially lower than previous measures.

DISCUSSION

Particle erosion

Using laser-diffraction analysis and microscopy, it can be confirmed that during dispersion in water, fine particles < 40 μm adhering to the surface of coffee particles are detached by the surrounding water flow. Regarding the total particle size distribution, a significant increase of the fine fraction is discernible. This effect of particle erosion was previously observed by Corrochano³² and stated to be relevant for extraction modeling by Ellero and Navarini.³⁵ A contribution by lipid droplets to the fine fraction can be neglected as the lipid content in coffee extracts is low compared to the volume of fine particles.³⁶ Moreover, this study revealed a remarkable increase in the fine fraction with an increase in extraction temperature. This positive correlation of the fine fraction with temperature refutes Corrochano's second hypothesis that the detected particles were lumps of solutes, which are soluble at higher temperatures. Instead, this research proposes that these fines are caused by particle erosion. It is assumed that the increase of solubility with increasing temperature,³ (e.g. valid for bitter components such as caffeine), leads to a higher pore accessibility and thus enables the release of more fine fragments into the liquid phase. Moreover, a reduction of the liquid's surface tension with extraction and temperature (according to the work of Navarini *et al.*³⁷) as well as the drop in water viscosity with rising temperature facilitates wetting

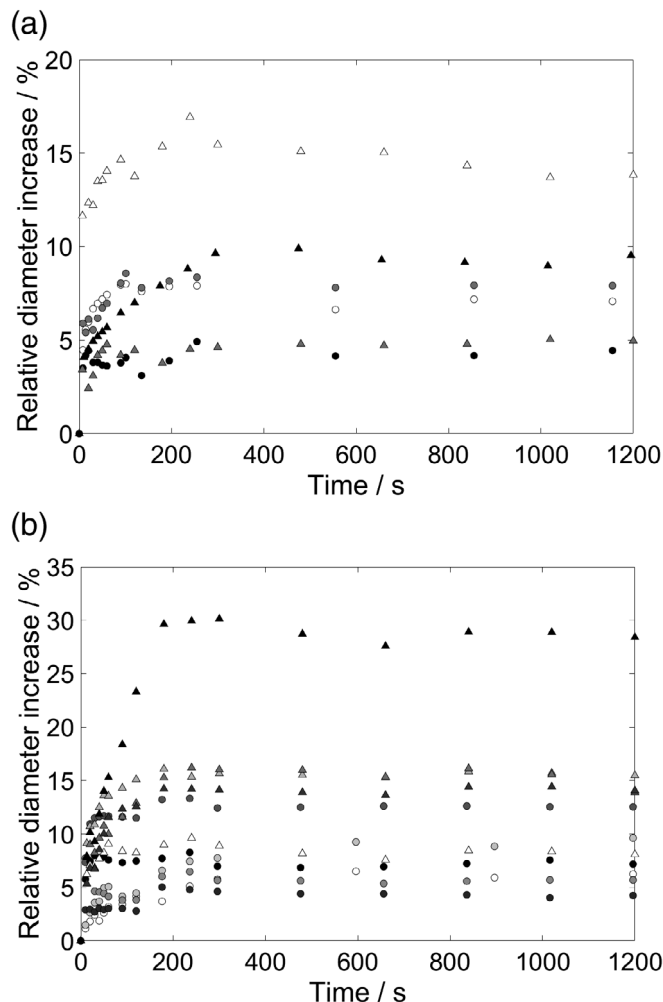


Figure 7 Relative diameter increase after different times of wetting at 80 °C (●) and at 25 °C (△). (a) Medium-roast coffee particles with initial diameters (in μm) of 608 (○), 519 (◐), 675 (●), 585 (△), 543 (▲), and 914 (▲). (b) Light-roast coffee particles with initial diameters (in μm) of 652 (○), 626 (◐), 462 (◑), 665 (●), 653 (◐), 547 (●), 472 (△), 589 (△), 520 (▲), 568 (▲), and 592 (▲).

and water ingress and probably enables more fragments to be washed from pores and capillaries. Accordingly, the effect of temperature on particle erosion must be taken into account – especially for filtration methods where fine particles have a strong influence on the specific cake filtration resistance.^{35,38}

Degree of swelling

Particle size distribution analysis yielded a total increase of the particle diameter by approximately 15%. This value is close to the results obtained by Spiro *et al.*²⁸ but is higher than the results from laser-diffraction analysis subsequently produced by other authors.^{13,31,32} This difference can be explained by the effect of particle erosion. The increase of the volume density for fine particle size classes connected with the simultaneous decrease for larger particle size classes leads to a change in the bimodal distribution, thereby affecting the value of the $d_{4,3}$. Thus, the $d_{4,3}$ (including all particle size classes) is underestimated along with the total increase calculated from the difference to the dry state. By previous sieving, air jet screening, and washing, the effect of particle erosion can be excluded – except for fine particles

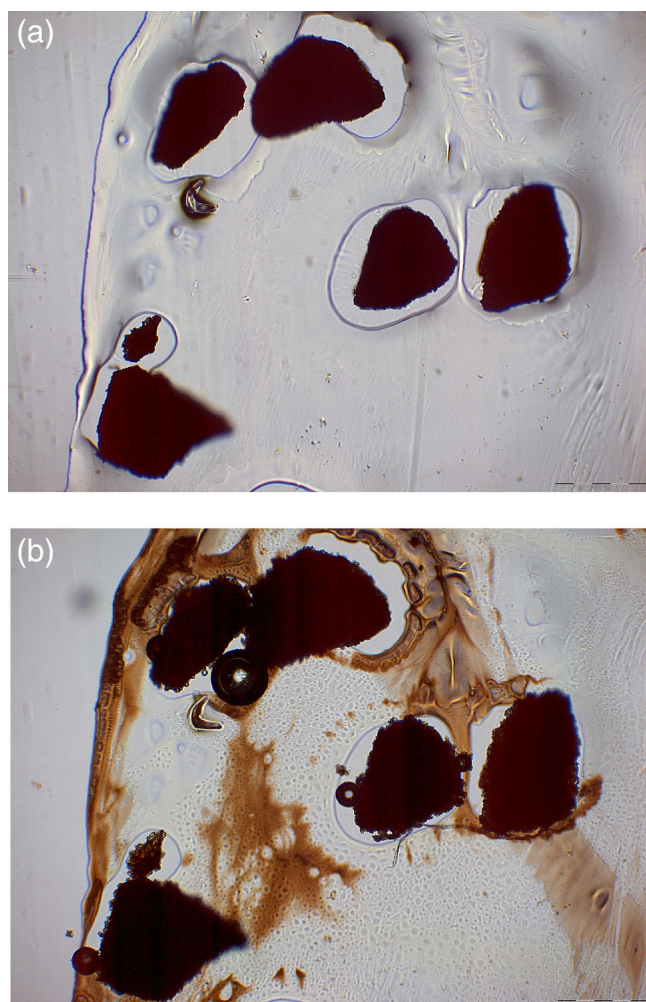


Figure 8 Light-roast particles in a dry and swollen state at 25 °C; gas bubbles and loosening fragments are visible at the surface of particles. (a) Before wetting. (b) After 20 min of wetting.

< 100 μm where separation efficiency was insufficient. This explains why this study's results for the total increase of the particle diameter are higher. Moreover, the analysis of cumulative distributions instead of the $d_{4,3}$ allowed an investigation of individual regions of the distributions and to exclude outliers at the distributions' left end, (which occurred due to residual fines and experimental error).

Influence of initial particle diameter and roasting degree

Neither by analysis of the particle size distribution nor by investigating individual particles under the microscope could a difference in swelling be seen with different initial particle diameters. An impact of the initial diameter (as might be assumed from Corrochano's³² results) does not seem to exist, which implies that the relative degree of swelling is not affected by grinding variations. The same applies to the roasting degree, as no significant difference was observed for light-roast coffee compared to medium roast. With regard to the content of insoluble polysaccharides, only the cellulose content remains virtually constant throughout roasting.¹⁸ Thus, it is hypothesized that cellulose has the highest influence on swelling according to the fact that no difference in swelling was observed for different roasting degrees at identical water quality and temperature.

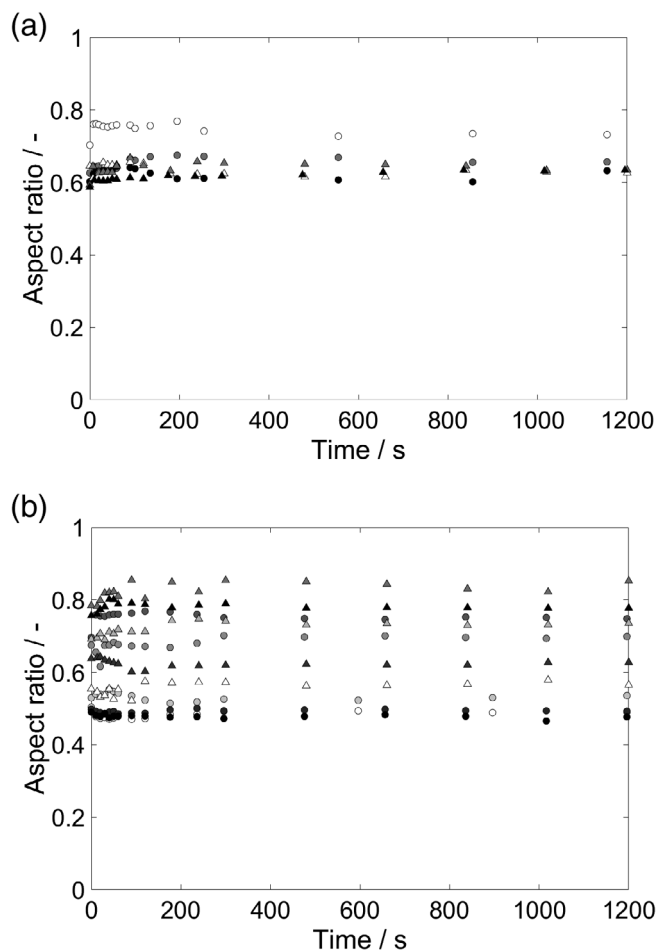


Figure 9 Aspect ratio after different times of wetting at 80 °C (○) and at 25 °C (△). (a) Medium-roast coffee particles with initial diameters (in μm) of 608 (○), 519 (●), 675 (●), 585 (△), 543 (△), and 914 (▲). (b) Light-roast coffee particles with initial diameters (in μm) of 652 (○), 626 (○), 462 (○), 665 (○), 653 (●), 547 (●), 472 (△), 589 (△), 520 (△), 568 (▲), and 592 (▲).

Time dependency of swelling

Image analysis revealed that the rate and final degree of swelling varies widely when comparing individual particles, which makes a verification of laser-diffraction measurements difficult. Additionally, the wide scattering of values and the appearance of gas bubbles complicated the investigation of influencing factors on swelling kinetics such as temperature and roasting degree. The large differences between single particles can be attributed to their individual physical structure, e.g. of pores and fibers, as well as their composition (depending on where the respective cells were located in the bean before grinding) and on the whole growth and processing history of the beans. To enable statistically significant results, vastly larger sample sizes would be needed, along with an automated method of analysis. However, it can be stated that swelling is quick and not negligible for the regular time of espresso brewing, as approximately 60–80% of the final diameter is reached after only 30 s. Regarding espresso extraction, however, it has to be considered that the effect of an elevated pressure on the swelling dynamics is not covered by this study and potential effects from this parameter require further investigations. With a typical duration of infusion brewing of around 4 min, it can be expected that swelling is completed according to the measurements in this research. Therefore, the

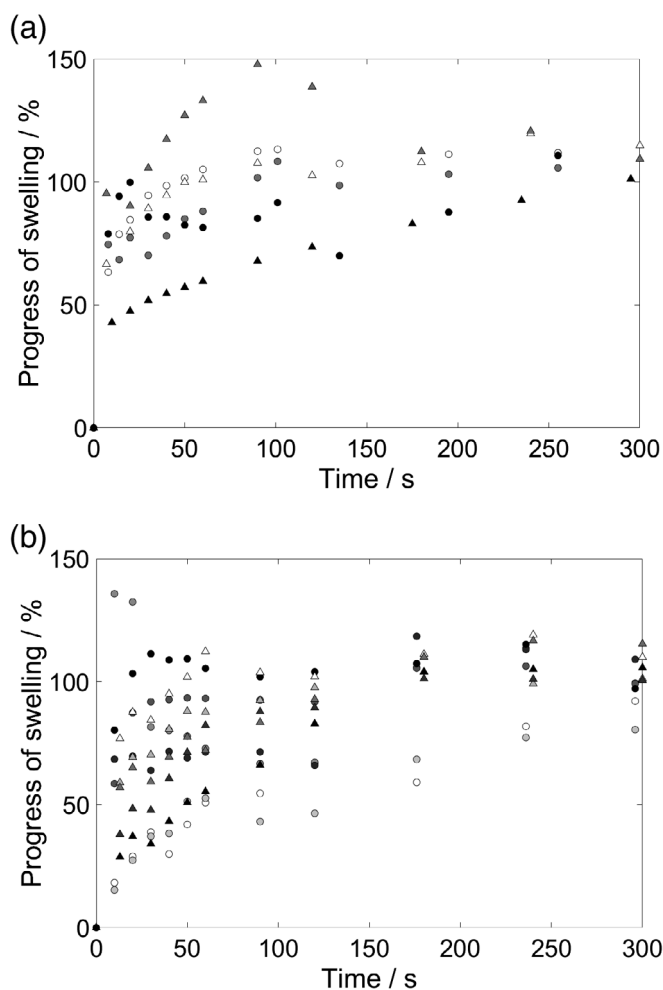


Figure 10 Progress of swelling after different times of wetting at 80 °C (○) and 25 °C (△). (a) Medium-roast coffee particles with initial diameters (in μm) of 608 (○), 519 (●), 675 (●), 585 (△), 543 (△), and 914 (▲). (b) Light-roast coffee particles with initial diameters (in μm) of 652 (○), 626 (○), 462 (○), 665 (●), 653 (●), 547 (●), 472 (△), 589 (△), 520 (△), 568 (▲), and 592 (▲).

swelling duration is expected to be distinctly shorter than that stated by Mateus *et al.*¹³

Furthermore, it can be concluded from the unchanged aspect ratio of particles and from visual observation (see Fig. 8) that coffee particles swell rather homogeneously, i.e. volume increase is isotropic and particle shape is barely influenced by swelling. This perception is consistent with the swelling behavior of cellulose being homogeneous in aqueous media.²⁵

CONCLUSIONS

Using laser diffraction analysis and microscopy, we have demonstrated that single particles of ground coffee swell distinctly as a consequence of wetting. The total size increase amounts to approximately 15%. The strong discrepancies in values measured by different authors in the past is traced back to the phenomenon of particle erosion which is increased with a rise in extraction temperature from 25 to 90 °C. A sieving method is proposed in this article to circumvent this distortion of the volume distribution.

The final degree of swelling is shown to be independent of the initial particle size. Our results are hence transferable to different

Table 2. Average progress of swelling after conventional brewing times

Water temperature	Progress of swelling	
	Medium roast	Light roast
30 s of wetting		
80 °C	83%	71%
25 °C	82%	59%
4 min of wetting		
80 °C	109%	101%
25 °C	111%	108%

grounds used for different brewing techniques. Two different conventional roasts have been compared with regard to their total degree of swelling. Both roasts exhibit the same size increase, leading to the conclusion that swelling is not influenced significantly by the roasting degree.

We furthermore reveal by measurements at different times after wetting that swelling is homogeneous in all directions and that it is completed within the first 4 min. A remarkable size increase already appears within the first 30 s. These findings emphasize the requirement of further research on potential effects from swelling on the extraction kinetics at specific extraction conditions.

ACKNOWLEDGEMENTS

Thanks to Fausto Kaffeerösterei GmbH, Munich, Germany, for supplying freshly roasted coffee beans. Special thanks go to the workshop of the Chair of Process Systems Engineering of Technical University of Munich for manufacturing the flow cell that has been used for microscopy and to Johann Landauer for providing valuable advice on particle analysis.

REFERENCES

- Voilley A, Sauvageot F, Simatos D and Wojcik G, Influence of some processing conditions on the quality of coffee brew. *J Food Process Pres* **5**:135–143 (1981).
- Andueza S, Maeztu L, Dean B, de Peña MP, Bello J and Cid C, Influence of water pressure on the final quality of arabica espresso coffee. Application of multivariate analysis. *J Agric Food Chem* **50**: 7426–7431 (2002).
- Andueza S, Maeztu L, Pascual L, Ibáñez C, de Peña MP and Cid C, Influence of extraction temperature on the final quality of espresso coffee. *J Sci Food Agric* **83**:240–248 (2003).
- Andueza S, Vila MA, Paz de Peña M and Cid C, Influence of coffee/water ratio on the final quality of espresso coffee. *J Sci Food Agric* **87**: 586–592 (2007).
- Gloss AN, Schönbacher B, Klopprogge B, D'Ambrosio L, Chatelain K, Bongartz A *et al.*, Comparison of nine common coffee extraction methods: instrumental and sensory analysis. *Eur Food Res Technol* **236**:607–627 (2013).
- Navarini L and Rivetti D, Water quality for espresso coffee. *Food Chem* **122**:424–428 (2010).
- Voilley A and Simatos D, Modeling the solubilization process during coffee brewing. *J Food Process Eng* **3**:185–198 (1979).
- Spiro M and Selwood RM, The kinetics and mechanism of caffeine infusion from coffee: the effect of particle size. *J Sci Food Agric* **35**: 915–924 (1984).
- Bear J, *Modeling Phenomena of Flow and Transport in Porous Media*. Springer International Publishing, Cham (2018).
- Kuhn M, Lang S, Bezold F, Minceva M and Briesen H, Time-resolved extraction of caffeine and trigonelline from finely-ground espresso

- coffee with varying particle sizes and tamping pressures. *J Food Eng* **206**:37–47 (2017).
- 11 Illy A and Viani R, *Espresso Coffee. The Science of Quality*, 2nd edn. Elsevier Academic, Amsterdam (2005).
 - 12 MacDougal DT and Spoehr HA, Growth and imbibition. *Proc Am Philos Soc* **56**:289–352 (1917).
 - 13 Mateus M-L, Rouvet M, Gummy J-C and Liardon R, Interactions of water with roasted and ground coffee in the wetting process investigated by a combination of physical determinations. *J Agric Food Chem* **55**:2979–2984 (2007).
 - 14 Wolfrom ML and Patin DL, Carbohydrates of the coffee bean. IV. An arabinogalactan 1. *J Org Chem* **30**:4060–4063 (1965).
 - 15 Wolfrom ML, Laver ML and Patin DL, Carbohydrates of the coffee bean. II. Isolation and characterization of a mannan 1. *J Org Chem* **26**:4533–4535 (1961).
 - 16 Wolfrom ML and Patin DL, Coffee constituents, isolation and characterization of cellulose in coffee bean. *J Agric Food Chem* **12**:376–377 (1964).
 - 17 Bradbury AG and Halliday DJ, Chemical structures of green coffee bean polysaccharides. *J Agric Food Chem* **38**:389–392 (1990).
 - 18 Thaler H and Arneth W, Untersuchungen an Kaffee und Kaffee-Ersatz. XIII Mitteilung Verhalten der Polysaccharid-Komplexe des rohen Arabica-Kaffees beim Rösten. *Zeitschrift für Lebensmittel-Untersuchung und Forschung* **140**:101–109 (1969).
 - 19 Asante M and Thaler H, Untersuchungen an Kaffee und Kaffee-Ersatz. XVII Verhalten der Polysaccharid-Komplexe von Robusta-Kaffee beim Rösten. *Zeitschrift für Lebensmittel-Untersuchung und Forschung* **159**:93–96 (1975).
 - 20 Sachslehner A, Foidl G, Foidl N, Gübitz G and Haltrich D, Hydrolysis of isolated coffee mannan and coffee extract by mannanases of *Sclerotium rolfsii*. *J Biotechnol* **80**:127–134 (2000).
 - 21 Grignon J and Scallan AM, Effect of pH and neutral salts upon the swelling of cellulose gels. *J Appl Polym Sci* **25**:2829–2843 (1980).
 - 22 Carlsson G, Kolseth P and Lindström T, Polyelectrolyte swelling behavior of chlorite delignified spruce wood fibers. *Wood Sci Technol* **17**:69–73 (1983).
 - 23 Eriksson I, Haglind I, Lidbrandt O and Sahnén L, Fiber swelling favoured by lignin softening. *Wood Sci Technol* **25**:135–144 (1991).
 - 24 Luukko K and Maloney TC, Swelling of mechanical pulp fines. *Cellulose* **6**:123–135 (1999).
 - 25 Cuissinat C and Navard P, Swelling and dissolution of cellulose, part III: plant fibres in aqueous systems. *Cellulose* **15**:67–74 (2008).
 - 26 Rivetti D, Navarini L, Cappuccio R, Abatangelo A, Petracco M and Suggi-Liverani F, Effect of water composition and water treatment on espresso coffee percolation. In ASIC Proceedings, 19th International Scientific Colloquium on Coffee, Trieste, Italy (2001).
 - 27 Sivetz M and Desrosier NW, *Coffee Technology*. AVI Publishing Company, Westport, CT (1979).
 - 28 Spiro M, Toumi R and Kandiah M, The kinetics and mechanism of caffeine infusion from coffee: the hindrance factor in intra-bean diffusion. *J Sci Food Agric* **46**:349–356 (1989).
 - 29 Hinz T, Steer A, Waldmann C, Cammenga HK and Eggers R, Röstkaffee-Extraktion: Einflußparameter und Modellierung. *Chem Ing Tech* **69**:685–690 (1997).
 - 30 Steer AG, *Physikalisch-chemische Parameter des Kaffeegetränkes und Untersuchungen zur Röstkaffee-Extraktion*, 1st edn. Cuvillier Verlag, Göttingen (2003).
 - 31 Hinz, T. Strukturbeschreibung disperser Naturstoffe als Grundlage für Modellentwicklungen. Doctoral Thesis, Technical University Hamburg, Hamburg (1997).
 - 32 Corrochano, B. R. Advancing the Engineering Understanding of Coffee Extraction. Doctoral Thesis, The University of Birmingham, Birmingham (2015).
 - 33 Spiro M and Chong YY, The kinetics and mechanism of caffeine infusion from coffee: the temperature variation of the hindrance factor. *J Sci Food Agric* **74**:416–420 (1997).
 - 34 Wang X and Lim L-T, A kinetics and modeling study of coffee roasting under isothermal conditions. *Food Bioproc Tech* **7**:621–632 (2014).
 - 35 Ellero M and Navarini L, Mesoscopic modelling and simulation of espresso coffee extraction. *J Food Eng* **263**:181–194 (2019).
 - 36 Ratnayake WMN, Hollywood R, O'Grady E and Stavric B, Lipid content and composition of coffee brews prepared by different methods. *Food Chem Toxicol* **31**:263–269 (1993).
 - 37 Navarini L, Ferrari M, Liverani FS, Liggieri L and Ravera F, Dynamic tensiometric characterization of espresso coffee beverage. *Food Hydrocoll* **18**:387–393 (2004).
 - 38 Hwang K-J and Lin I-L, Effects of mixing ratio of binary fine particles on the packing density and filtration characteristics. *KONA Powder Part J* **33**:296–303 (2016).

APPENDIX

STATISTICAL ANALYSIS RESULTS

In this appendix, the results from statistical tests are presented supporting our statements in the Results section. The *P*-values of the two-sample *t*-tests, Mann–Whitney U-tests, and ANOVA are listed as well as the slopes from linear regressions.

Compared parameters	Range of size classes (µm)	Difference of means ^a	P-Value	
			t-Test	Mann–Whitney
Dry <i>versus</i> wet	0.5–31	< 0	< 0.01	< 0.01
	31–60	> 0	> 0.01 ^b	> 0.01
	60–250	< 0	< 0.01 ^c	< 0.01
	250–730	> 0	< 0.01	< 0.01
	730–1750	≤ 0	> 0.01 ^d	> 0.01
25 °C <i>versus</i> 90 °C	0.5–50	< 0	< 0.01	< 0.01
	50–90	< 0 or > 0	> 0.01	> 0.01
	90–510	> 0	< 0.01	< 0.01
	510–1750	≤ 0 or > 0	> 0.01	> 0.01

^a Difference is calculated as mean of first parameter minus mean of second parameter, i.e. dry minus wet and 90–25 °C.
^b Except for 31–37 µm: *P* < 0.01.
^c Except for 210–250 µm: *P* > 0.01.
^d Except for 730–870 µm: *P* < 0.01.

	Slope × 10 ⁻³ (% µm ⁻¹)	P-Value
Medium roast	-2.95	0.291
Light roast	-2.54	0.498

Compared parameters	Identical parameters	P-Value	
		t-Test	Mann–Whitney
25 °C <i>versus</i> 80 °C	Medium roast	0.372	0.400
	Light roast	0.065	0.017
Medium roast <i>versus</i> light roast	80 °C	0.517	0.905
	25 °C	0.173	0.143

	80 °C			25 °C		
	<i>d</i> ₀ (µm)	Slope × 10 ⁻⁵ (s ⁻¹)	<i>P</i> -Value	<i>d</i> ₀ (µm)	Slope × 10 ⁻⁵ (s ⁻¹)	<i>P</i> -Value
Medium roast	608	-2.11	0.100	585	-1.63	0.095
	519	1.62	0.171	543	0.660	0.559
	675	-1.24	0.250	914	2.84	4.35 × 10 ⁻⁶
Light roast	652	1.26	0.088	472	2.51	0.025
	626	-0.723	0.392	589	2.78	0.013
	462	3.37	0.008	520	2.97	0.051
	665	-0.292	0.788	568	-0.291	0.706
	653	0.368	0.206	592	-0.344	0.667
	547	-0.621	0.075			